IEEE Access
Multidisciplinary | Rapid Review | Open Access Journal

Received February 23, 2019, accepted March 7, 2019, date of publication March 18, 2019, date of current version April 8, 2019.

Digital Object Identifier 10.1109/ACCESS.2019.2905855

A Dual-Band Balanced-to-Balanced Power Divider With High Selectivity and Wide Stopband

LEI CHEN[1], FENG WEI[2], (Member, IEEE), XING YU CHENG[2], AND QIN KUN XIAO[1]
[1]School of Electronic and Information Engineering, Xi'an Technological University, Xi'an 710021, China
[2]National Key Laboratory of Antennas and Microwave Technology, School of Electrical Engineering, Xidian University, Xi'an 710071, China

Corresponding author: Lei Chen (sumter1108@163.com)

This work was supported in part by the National Natural Science Foundation of China (NSFC) under Grant 61671362, in part by the Natural Science Foundation of Shaanxi Province under Grant 2017JM6041, in part by the Fundamental Research Funds for the Central Universities under Grant JB180204, and in part by the State Key Laboratory of Metamaterial Electromagnetic Modulation Technology.

ABSTRACT A dual-band balanced-to-balanced (BTB) filtering power divider (FPD) is presented, which can achieve an in-phase power division with high selectivity. The proposed FPD is composed of microstrip-to-slotline transition structures (MTSTSs), T-shaped slotline, and multiple stub-loaded resonators (SLRs). A dual-band differential-mode (DM) response with a steep filtering performance is generated by employing SLRs. By adjusting the electrical lengths of SLRs and the gaps between each resonator and microstrip lines, the fractional bandwidth (FBW) is controllable. By introducing slotline resonators loaded with surface-mounted resistors, the isolation between the two output ports is increased. Meanwhile, a wide DM stopband with a high rejection level is obtained. Moreover, good wideband common-mode (CM) suppression is achieved intrinsically, thereby simplifying the design procedure greatly. To verify the theoretical prediction, one FPD prototype is fabricated. A good agreement between the simulated and measured results is observed. To the best of authors' knowledge, the proposed dual-band BTB FPD is first ever reported.

INDEX TERMS Balanced-to-balanced (BTB), common-mode suppression, dual-band, filtering power divider, stub-loaded resonator (SLR).

I. INTRODUCTION

Compared with the conventional single-ended components, balanced counterparts show more advantages due to their higher immunity to electromagnetic interferences and reliability. In order to integrate the active balanced circuits and differential antennas to build up fully balanced transceivers, some balanced passive components have been presented, including balanced-to-balanced (BTB) bandpass filters (BPFs)/power dividers (PDs). On the other hand, as multi-band wireless communication systems are commonplace, multi-band balanced components are highly needed. In the past ten years, some balanced BPFs and PDs have been designed [1]–[8]. In [4], a balanced wideband network with unequal power division and broadband common mode (CM) suppression was achieved. Wideband PDs obtaining a high CM suppression were realized by etching the slot on the ground of Wilkinson PD [5], [6]. A differential PD with a small size based on coupled microstrip line was proposed in [7]. A balanced PD with 1-to-2^n way was implemented in [8]. Recently, in order to achieve miniaturization, many PDs integrated filtering response, called filtering PDs (FPDs), are emerging, which can achieve the functions of filters and PDs simultaneously [9]–[12]. Some balanced-to-single-ended (BTSE) FPDs based on the coupled lines and branch lines were proposed in [13] and [14], respectively. Recently, a dual-band BTSE FPD based on coupled ring resonators were proposed in [15]. To the author's best knowledge, however, there is no research work on BTB dual-band FPD published.

In this paper, a dual-band BTB FPD is implemented by employing stub-loaded resonators (SLRs). The center frequencies and bandwidths of the differential-mode (DM) responses can be tuned by controlling the dimensions of SLRs. It is found that the proposed FPD can achieve independent CM responses with a larger bandwidth and a higher suppression. In addition, by adopting slotline resonators loaded with surface-mounted resistors, the isolation between the two output ports is improved obviously. The proposed FPD is designed on the substrate Rogers RT/Duroid 5880 ($\varepsilon_r = 2.2$, $h = 0.8$ mm, $\tan\delta = 0.0009$).

The associate editor coordinating the review of this manuscript and approving it for publication was Jiansong Liu.

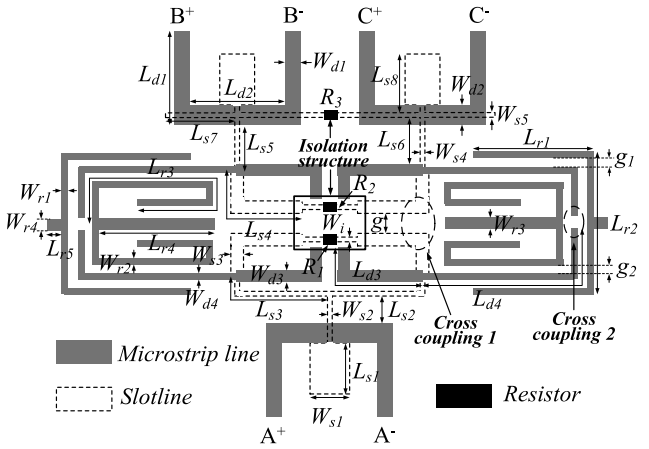

FIGURE 1. Configuration of the proposed BTB dual-band FPD.

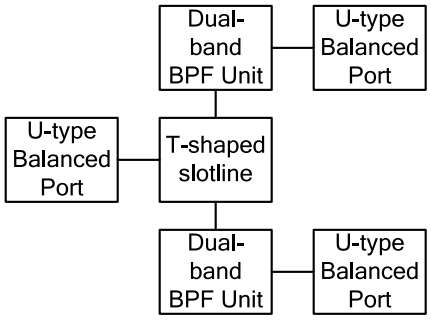

FIGURE 2. Diagram of the proposed FPD.

Compared to the reported works, including our previous works [16], the contributions of the proposed FPD in this paper are follows. Firstly, a balanced-to-balanced FPD with dual-band DM response is proposed. To the best of authors' knowledge, the proposed dual-band BTB FPD is first ever reported. Secondly, a new isolation method is proposed to improve the isolation between the output ports. Previous isolation method for single-band BTB FPD are not suitable for the dual-band one. Three pairs of uniform impedance slotline loaded with surface-mounted resistors are employed. Thirdly, the proposed structure has a great flexibility to indenpendtly change the two center frequencies and the bandwidths, respectively, to meet different system requirements. Fourthly, a wide DM stopband with a high rejection level is obtained.

II. BALANCED DUAL-BAND FPD

A. OVERALL STRUCTURE

A traditional slotline is a planar transmission line. It consists of a dielectric substrate with a narrow slot etched in the metallization on one side of the substrate. The other side of the substrate is without any metallization. The configuration of the proposed BTB dual-band FPD is shown in Fig. 1. Fig. 2 shows the diagram of the proposed FPD, which consists of balanced input/output U-type microstrip-to-slotline transition structures (MTSTSs), T-shaped slotline and filtering

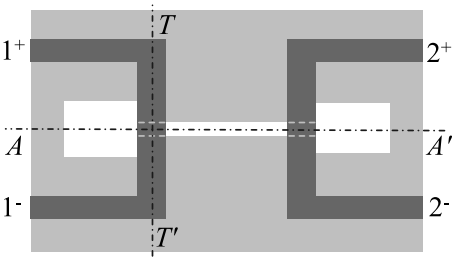

FIGURE 3. Configuration of the balanced MSTS.

units. Each MTSTS is composed of a U-type microstrip line and a stepped-impedance slotline resonator. The slotline on the ground plane of a substrate is crossed at a right angle with a U-type microstrip line on its opposite interface. Meanwhile, the slotline resonator extends about a quarter of wavelength beyond the U-type microstrip line. In order to obtain a miniaturization of the proposed balanced filtering power divider, stepped-impedance slotlines are adopted, which are similar to the stepped-impedance resonator (SIR). Because of the geometrical symmetry, the balanced MTSTS can be analyzed using the DM and CM method, as shown in Fig. 3. Under a DM operation, the symmetrical plane *A-A'*becomes a perfectly electric wall so that the electric field in the DM feeding line is in analog to the slotline [17], as shown in Fig. 4(a). Through strong magnetic coupling, the DM signals along the microstrip lines can be transmitted to the slotline and a wide passband under the DM operation can be achieved. By employing two pairs of symmetry L-shaped MTSTSs and two pair of SLRs, the proposed FPD can achieve a steep dual-band bandpass response. Finally, two DM signals with the equal magnitude and phase propagating along the slotline can be transmitted successfully into the two output ports by MTSTS again. When a CM excitation is applied, a virtual magnetic wall at *T-T'* plane is formed, which is perpendicular to the electric field of the slotline mode, thereby realizing a better CM suppression, as shown in Fig. 4(b). Since the CM signals are intrinsically suppressed, only the DM passband response needs to be considered in the design process, which decreases the design difficulties greatly.

B. BANDPASS RESPONSES

The proposed dual-band BTB FPD can realized a good dual-band bandpass response by employing a pair of symmetrical L-shaped MTSTSs and two SLRs in each sub-circuit of T-shaped slotline. The employed SLR is composed of a half wavelength microstrip resonator and an open-stub loaded at the center, as shown in Fig. 5(a). Since SLR is symmetrical in structure, odd- and even-mode analysis can be adopted to analyze it, as shown in Fig. 5 (b) and (c). For the odd-mode excitation, there is a voltage null along the middle of the resonator. Therefore, the odd-mode resonant frequencies can be easily as:

$$f_{odd} = \frac{(2n-1)c}{2L_1\sqrt{\varepsilon_{eff}}} \tag{1}$$

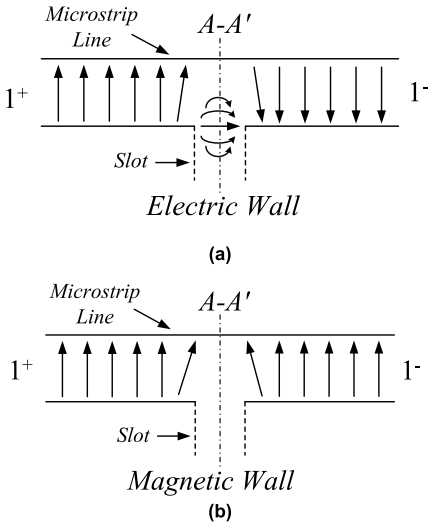

FIGURE 4. Cross-sectional views of electrical field distribution at T-T' plane. (a) DM feeding. (b) CM feeding.

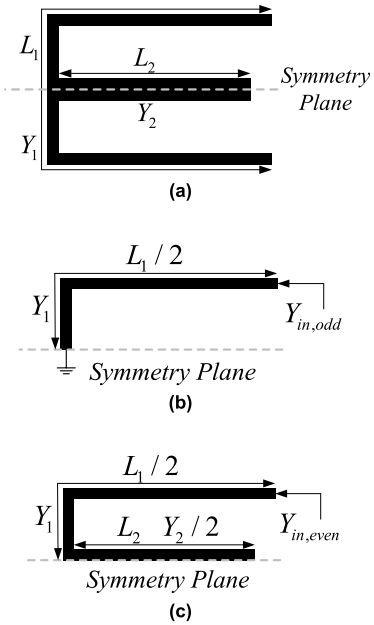

FIGURE 5. (a) Layout of SLR. (b) Odd-mode subcircuit model and (c) Even-mode subcircuit model.

where $n = 1, 2, 3, \ldots$, c is the speed of light in free space, and ε_{eff} denotes the effective dielectric constant of the substrate. It can be observed that the odd-mode resonant frequencies are not affected by the open stub.

For the even-mode excitation, there is no current flow through the symmetrical plane. The even-mode resonant frequencies for the case of $Y_2 = 2Y_1$ can thus be attained as:

$$f_{even} = \frac{nc}{(L_1 + 2L_2)\sqrt{\varepsilon_{eff}}} \tag{2}$$

According to the analysis above, the adopted SLR has two fundamental resonant frequencies. When $n = 1$, the two

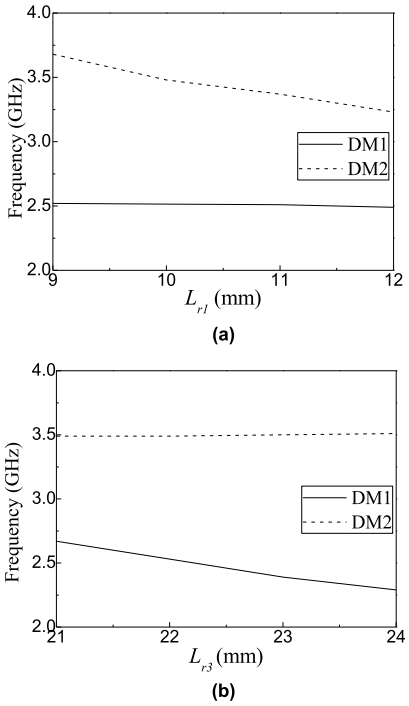

FIGURE 6. Simulated DM frequency responses of the proposed dual-band BTB FPD with different (a) L_{r1} and (b) L_{r3}.

fundamental resonant frequencies can be expressed as:

$$f_1 = f_{odd} = \frac{c}{2L_1\sqrt{\varepsilon_{eff}}} \tag{3}$$

$$f_2 = f_{even} = \frac{c}{(L_1 + 2L_2)\sqrt{\varepsilon_{eff}}} \tag{4}$$

It is easy to control the center frequencies and bandwidths of the proposed dual-band BTB FPD to meet different requirements. The effects of the dimensions on the DM and CM frequency responses are analyzed by EM simulation software HFSS 13.0. It can be observed from Fig. 6 that both the two DM frequencies can be controlled independently by L_{r1} and L_{r3}, respectively. The CM responses remain almost unchanged with these two parameters, which means that the DM responses are independent with the CM ones, as shown in Fig. 7.

The proposed structure has a great flexibility to control the bandwidths of the two passbands. The first method is to control the couplings between the feeding line and each resonator, respectively. The tight coupling will result into a wide passband while the weak coupling will realize a narrow passband. The second method is to control the spacing between the two resonant frequencies of each resonator, which is controlled by the length of the open-stub loaded at the center of SLR. It can be noted that the bandwidth is easy to control by adjusting the interval between f_1 and f_2. Large frequency spacing leads to a wide bandwidth. By properly adjusting the interval of two resonances of each SLR, two controllable bandwidths of the DM passbands can be achieved. The bandwidths of the two DM frequencies are

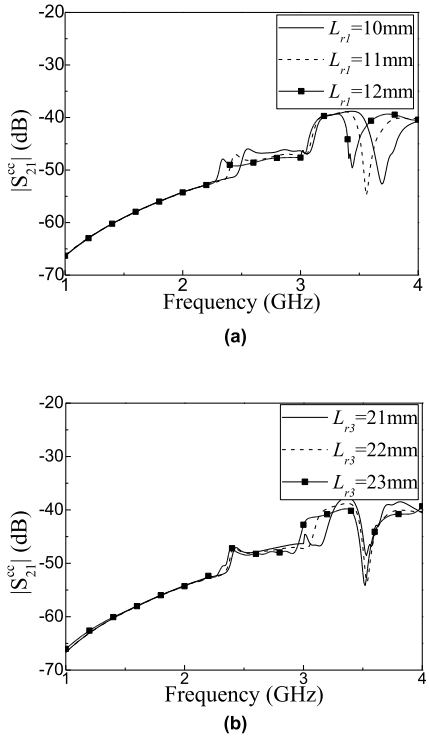

FIGURE 7. Simulated DM frequency responses of the proposed dual-band BTB FPD with different (a) L_{r1} and (b) L_{r3}.

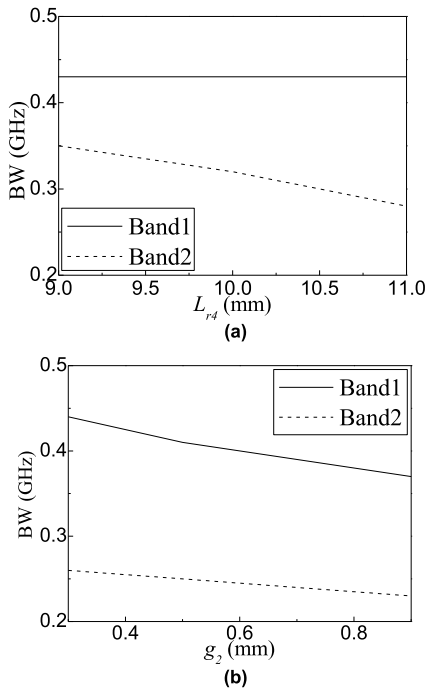

FIGURE 8. Effects of (a)L_{r4} and (b)g_2 on the DM bandwidths of the proposed dual-band BTB FPD.

decreased as g_2 increases, as shown in Fig. 8 (b). However, only the bandwidth of the 2nd DM frequency changes with L_{r4}, as shown in Fig. 8 (a). Furthermore, the bandwidth of the two DM frequencies can also be tuned by changing g_1 and

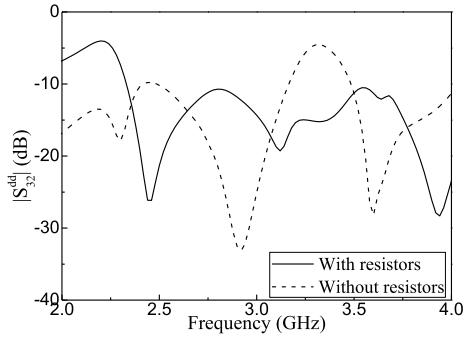

FIGURE 9. Comparison of DM isolation between the two output ports with and without resistors.

TABLE 1. Comparisons with some reported FPDs.

	f_0 (GHz)	Input/Output Type	Insertion Loss (dB)	$\lvert S_{21}^{cc}\rvert$ (dB)	Size (λ_g^2)
Ref[10]	1.88	BTSE	0.7	21	0.3×1.1
Ref[11]	2.82/ 3.22	BTSE	Not given	>18	0.9×0.53
Our work	2.5/ 3.5	BTB	0.53/0.72	> 36	0.6×0.47

L_{r5}, respectively. Meanwhile, in order to improve the selectivity of the bandpass response greatly, three transmission zeros (TZs) are achieved. By taking advantage of cross coupling 1 between the slotlines, which locate below the L-shaped microstrip lines, as shown in Fig. 1, TZ_1 can be realized at the lower frequency outside the 1st passband. TZ_2 is realized due to the cross coupling 2 between the L-shaped microstrip lines. TZ_3 is generated because of the intrinsic characteristics of the embedded SLRs. The effects of dimensions on TZs are not given here due to the length of the paper.

C. ISOLATION

In the previous work, one isolation method was proposed in [16], which can only be used to improve the isolation with one passband not for the dual-band FPD. Therefore, a novel isolation structure based on slotlines loaded with resistors across the midpoint of each slotline is proposed, as shown in Fig. 1, which is composed of three pairs of uniform impedance slotline connected the two sub-circuits of the T-shaped slotline and resistors connected across the midpoint of the slotlines. The improved passbands isolation performance can be clearly seen in Fig. 9. Finally, by adopting the befitting design and optimizing method, a balanced-to-balanced in-phase FPD with high selectivity and improved isolation performance can be realized.

III. FPD DESIGN AND DISCUSSION

To verify the theoretical prediction, a dual-band BTB FPD was fabricated and measured with an Agilent VNA (vector network analyzer) N5230A. All the dimensions are optimized as follows: $W_{d1} = W_{d2} = 2.5$ mm, $W_{d3} = 1.2$ mm,

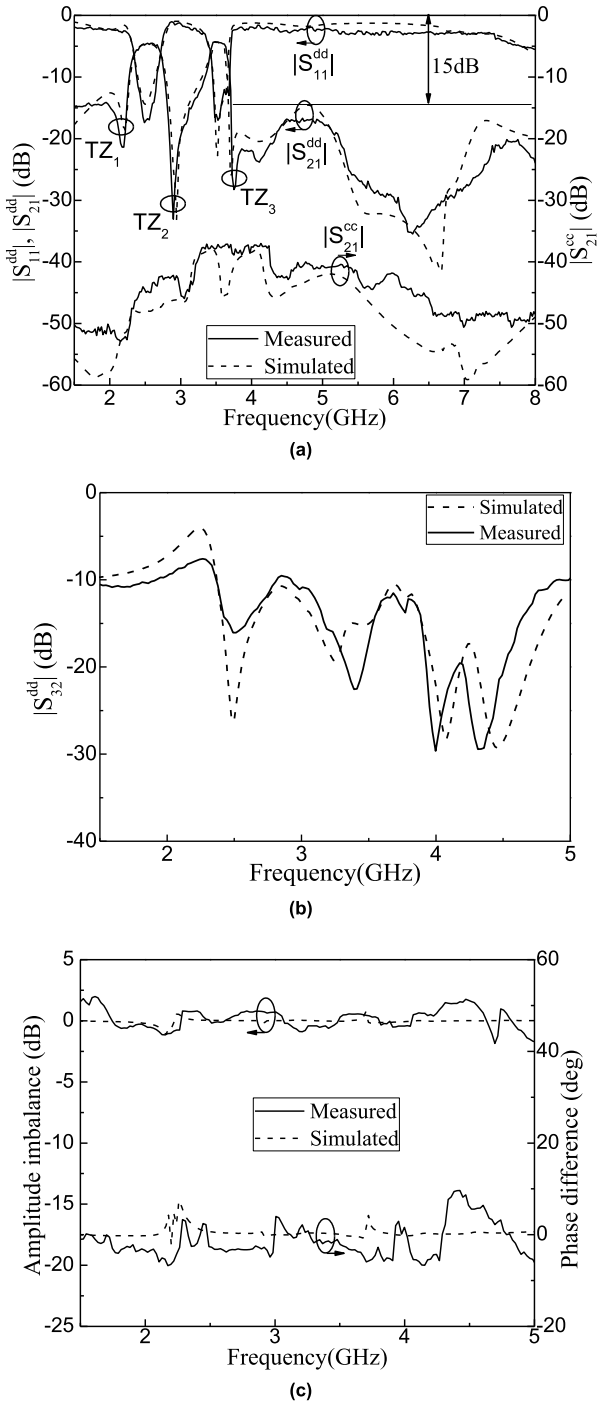

FIGURE 10. Simulation and measurement of the proposed dual-band BTB FPD. (a) DM return loss and DM/CM insert loss, (b) DM isolation and (c) DM amplitude imbalance and phase difference between the two output ports.

$W_{d4} = 0.5$ mm, $W_{r1} = W_{r2} = 0.5$ mm, $W_{r3} = 0.6$ mm, $W_{r4} = 0.5$ mm, $W_{s1} = 6.0$ mm, $W_{s2} = 0.2$ mm, $W_{s3} = 1.0$ mm, $W_{s4} = 0.2$ mm, $W_{s5} = 0.15$ mm, $W_i = 0.2$ mm, $L_{d1} = 14$ mm, $L_{d2} = 12$ mm, $L_{d3} = 14.6$ mm, $L_{d4} = 17.3$ mm, $L_{r1} = 11$ mm, $L_{r2} = 12.4$ mm, $L_{r3} = 24.8$ mm, $L_{r4} = 10.3$ mm, $L_{s1} = 8.0$ mm, $L_{s2} = 3.0$ mm, $L_{s3} = 15.4$ mm, $L_{s4} = 13.7$ mm, $L_{s5} = 4.0$ mm,

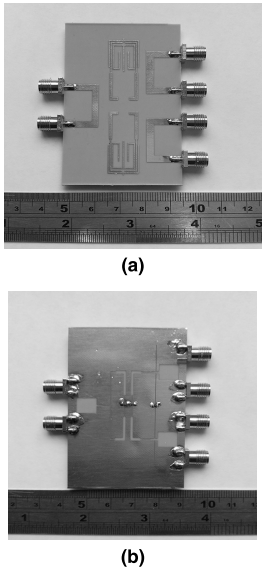

FIGURE 11. Photograph of the fabricated dual-band BTB FPD. (a) Top view and (b) Bottom view.

$L_{s6} = 5.725$ mm, $L_{s7} = 10.3$ mm, $L_{s8} = 9.125$ mm, $g_1 = 0.25$ mm, $g_2 = 0.4$ mm, $g = 2$ mm, $R_1 = 100\Omega$, $R_2 = 100\Omega$,$R_3 = 20\Omega$ (0402 surface-mounted package, from *MuRata* Corporation). Fig. 10 shows the comparison of the simulation and measurement of the proposed dual-band BTB FPD. The measured two DM passbands are centered at 2.5 and 3.5 GHz, respectively, with a 3-dB fractional bandwidth (FBW) of 17.2% and 9.3%. The measured minimum insertion losses of the two DM passbands are 1.53 and 1.33 dB, respectively (the 3 dB power division intrinsic loss is not included), and the return losses are greater than 17 dB within the operating bands. Moreover, the stopband can be expanded to 8.0 GHz with a large rejection level of 15 dB, which is 3.2 times of the fundamental frequency. The measured minimum isolation is larger than 13 dB. The measured amplitude imbalance and phase difference between the two balanced output ports are less than 0.5 dB and 5° in the two DM passbands, respectively. In addition, the measured CM suppression are greater than 36 dB for both passbands. A comparison of the performances between the proposed dual-band BTB FPD and other ones is shown in Table 1. It can be seen that the proposed FPD has better DM/CM responses and a smaller size. Fig. 11 shows the photograph of the fabricated dual-band BTB FPD.

IV. CONCLUSION

In this paper, a BTB two-way in-phase filtering power divider has been designed. The proposed dual-band FPD has a great flexibility in DM responses. In addition, a high and broadband CM suppression is achieved without using any additional stubs, thereby making the FPD electrically small. The planar structure, good performance and compact size make the proposed BTB dual-band FPD suitable for applications to multimode balanced communication systems.

REFERENCES

[1] J. Shi and Q. Xue, "Balanced bandpass filters using center-loaded half-wavelength resonators," *IEEE Trans. Microw. Theory Techn.*, vol. 58, no. 4, pp. 970–977, Apr. 2010.

[2] J.-X. Chen, M.-Z. Du, Y.-L. Li, Y.-J. Yang, and J. Shi, "Independently tunable/controllable differential dual-Band bandpass filters using element-loaded stepped-impedance resonators," *IEEE Trans. Compon., Packag., Manuf. Technol.*, vol. 8, no. 1, pp. 113–120, Jan. 2018.

[3] F. Wei, P.-Y. Qin, Y. J. Guo, C. Ding, and X. W. Shi, "Compact balanced dual- and tri-band BPFs based on coupled complementary split-ring resonators (C-CSRR)," *IEEE Microw. Wireless Compon. Lett.*, vol. 26, no. 2, pp. 107–109, Feb. 2016.

[4] W. Feng, C. Zhao, W. Che, and Q. Xue, "A balanced-to-balanced network with unequal power division and wideband common mode suppression," *IEEE Microw. Wireless Compon. Lett.*, vol. 26, no. 4, pp. 237–239, Apr. 2016.

[5] J. Shi, J. Wang, K. Xu, J.-X. Chen, and W. Liu, "A balanced-to-balanced power divider with wide bandwidth," *IEEE Microw. Wireless Compon. Lett.*, vol. 25, no. 9, pp. 573–575, Sep. 2015.

[6] F. Wei, X. B. Zhao, X. Y. Wang, B. Li, and X. W. Shi, "Balanced UWB power divider with one narrow notch-band," *Electron. Lett.*, vol. 53, pp. 1524–1526, Nov. 2017.

[7] J. Shi and K. Xu, "Compact differential power divider with enhanced bandwidth and in-phase or out-of-phase output ports," *Electron. Lett.*, vol. 50, no. 17, pp. 1209–1211, Aug. 2014.

[8] J. Shi, K. Xu, W. Zhang, J.-X. Chen, and G. Zhai, "An approach to 1-to-2^n way microstrip balanced power divider," *IEEE Trans. Microw. Theory Techn.*, vol. 64, no. 12, pp. 4222–4231, Dec. 2016.

[9] X. Gao, W. Feng, W. Che, and Q. Xue, "Wideband balanced-to-unbalanced filtering power dividers based on coupled lines," *IEEE Trans. Microw. Theory Techn.*, vol. 65, no. 1, pp. 86–95, Jan. 2017.

[10] K. Xu, J. Shi, L. Lin, and J.-X. Chen, "A balanced-to-unbalanced microstrip power divider with filtering function," *IEEE Trans. Microw. Theory Techn.*, vol. 63, no. 8, pp. 2561–2569, Aug. 2015.

[11] W. Feng, M. Hong, and W. Che, "Dual-band balanced-to-unbalanced filtering power divider by coupled ring resonators," *Electron. Lett.*, vol. 52, no. 22, pp. 1862–1864, Oct. 2016.

[12] X. Wang, J. Wang, W.-W. Choi, L. Yang, and W. Wu, "Dual-wideband filtering power divider based on coupled stepped-impedance resonators," *IEEE Microw. Wireless Compon. Lett.*, vol. 28, no. 10, pp. 873–875, Dec. 2018.

[13] X. Wang, J. Wang, G. Zhang, J.-S. Hong, and W. Wu, "Dual-wideband filtering power divider with good isolation and high selectivity," *IEEE Microw. Wireless Compon. Lett.*, vol. 27, no. 12, pp. 1071–1073, Dec. 2017.

[14] G. Zhang, J. Wang, L. Zhu, and W. Wu, "Dual-band filtering power divider with high selectivity and good isolation," *IEEE Microw. Wireless Compon. Lett.*, vol. 26, no. 10, pp. 774–776, Oct. 2016.

[15] C. Cai, J. Wang, Y. Deng, and J.-L. Li, "Design of compact dual-mode dual-band filtering power divider with high selectivity," *Electron. Lett.*, vol. 51, no. 22, pp. 1795–1796, Oct. 2015.

[16] F. Wei, Z.-J. Yang, P.-Y. Qin, Y. Jay Guo, B. Li, and X.-W. Shi, "A balanced-to-balanced in-phase filtering power divider with high selectivity and isolation," *IEEE Trans. Microw. Theory Techn.*, vol. 67, no. 2, pp. 683–694, Feb. 2019.

[17] X. Guo, L. Zhu, and W. Wu, "Strip-loaded slotline resonators for differential wideband bandpass filters with intrinsic common-mode rejection," *IEEE Trans. Microw. Theory Techn.*, vol. 64, no. 2, pp. 450–458, Feb. 2016.

Authors' photographs and biographies not available at the time of publication.